

# ESR Detection of optical dynamic nuclear polarization in GaAs/Al<sub>x</sub>Ga<sub>1-x</sub>As quantum wells at unity filling factor in the quantum Hall effect

Sergey A. Vitkalov\* and C. Russell Bowers†

*Chemistry Department, University of Florida, Gainesville, Florida 32611-7200*

Jerry A. Simmons and John L. Reno

*Sandia National Laboratories, MS 1415, Albuquerque, New Mexico 87185-1415*

(Received 12 October 1998)

This paper presents a study of the enhancement of the Zeeman energy of two-dimensional (2D) conduction electrons near the  $\nu=1$  filling factor of the quantum Hall effect by optical dynamic nuclear polarization. The change in the Zeeman energy is determined from the Overhauser shift of the transport detected electron spin resonance in GaAs/Al<sub>x</sub>Ga<sub>1-x</sub>As multiquantum wells. In a separate experiment the NMR signal enhancement factor is obtained by radio frequency detected nuclear magnetic resonance under similar conditions in the same sample. These measurements afford an estimation of the hyperfine coupling constant between the nuclei and 2D conduction electrons.

## I. INTRODUCTION

Recently the quantum Hall effect (QHE) at filling factor  $\nu=1$  has received much interest following the discovery of a new type of spin order in the two-dimensional electron system (2DES) of Al<sub>x</sub>Ga<sub>1-x</sub>As/GaAs quantum well structures.<sup>1</sup> Experimental investigations<sup>2-8</sup> have largely substantiated theoretical predictions<sup>9-11</sup> that charged spin texture excitations (i.e., Skyrmions) can occur in the vicinity of  $\nu=1$  and other integer and fractional fillings under certain conditions. According to theory, the relevant parameter governing the number of spin flips associated with the excitation is the dimensionless Zeeman energy  $\tilde{g} \equiv |g \gamma_e| \hbar B_0 / (e^2 / \epsilon l_0)$ , where  $g \approx -0.4$  is the single electron Landé  $g$  factor,  $\gamma_e$  is the electron gyromagnetic ratio (a negative quantity),  $l_0 = (\hbar / e B_\perp)^{1/2}$  is the magnetic length,  $\epsilon$  is the dielectric constant of GaAs, and  $B_\perp$  is the component of the total magnetic field  $B_0$  normal to the 2DES. To study these ground-state excitations, several different methods have been employed to control  $\tilde{g}$ . For example, the  $g$  factor can be reduced by the application of hydrostatic pressure<sup>12</sup> or by the addition of aluminum.<sup>13</sup> However, these techniques result in a considerable reduction in the electron density and a severe degradation of the 2D electron mobility. Alternatively,  $\tilde{g}$  can be controlled by the tilted field method,<sup>5,14-18</sup> but this method also has several fundamental drawbacks: (i) it can only increase  $\tilde{g}$ , (ii) Landau level mixing or subband energy changes can be introduced when  $B_\perp$  or  $B_0$  are varied,<sup>19</sup> (iii) the temperature must be varied to measure the activation energy.

Ideally, one would like to be able to change  $\tilde{g}$  while keeping the temperature and external field  $B_0$  constant. One possibility is to use the local nuclear hyperfine field,  $B_n$ , resulting in a total Zeeman energy  $E_z = g \gamma_e \hbar (B_0 + B_n)$ , where<sup>20</sup>

$$B_n = \frac{8\pi}{3} g \sum_j a^{(j)} \gamma_n^j |\psi(r^{(j)})|^2 \langle I_z^{(j)} \rangle \quad (1)$$

is summed over all isotopes (i.e., <sup>69</sup>Ga, <sup>71</sup>Ga, and <sup>75</sup>As), each with natural abundance  $a^{(j)}$ , gyromagnetic ratio  $\gamma_n^{(j)}$ , and nuclear spin expectation value  $\langle I_z^{(j)} \rangle$  along the  $z$  axis. In the context of electron spin resonance (ESR),  $B_n$  is known as the Overhauser shift.<sup>21</sup> In this paper we report the enhancement of  $E_z$  for 2D conduction electrons near the  $\nu=1$  filling factor in the QHE regime by optical dynamic nuclear polarization (DNP). The change in the Zeeman energy is determined from the Overhauser shift of the transport detected ESR in GaAs/Al<sub>x</sub>Ga<sub>1-x</sub>As multiquantum wells. Furthermore, we obtain the NMR signal enhancement factor by radio frequency detected NMR under similar conditions in the same sample. These measurements allow us to estimate the hyperfine coupling constant between the nuclei and 2D conduction electrons.

In the absence of the spin-orbit interaction, as in the conduction band of GaAs, neither the cyclotron energy nor the electron-electron Coulomb interactions are affected by  $B_n$ , regardless of its magnitude and sign, because the origin of  $B_n$  is the contact interaction between the electron and nucleus.<sup>22</sup> In semiconductors, the nuclear spin polarization  $\langle I_z \rangle$  can be dramatically enhanced by microwave<sup>20,22,23</sup> or optical DNP.<sup>24-30</sup> Enhancement of  $B_n$  has been previously reported in a variety of homogeneous and heterogeneous semiconductor systems. In bulk GaAs, optical DNP enhancement of  $B_n$  causes the Hanle curve for depolarization of the shallow donor trapped electron-hole recombination photoluminescence to be displaced from zero field.<sup>31,32</sup> In Al<sub>x</sub>Ga<sub>1-x</sub>As/GaAs quantum dots, optical DNP enhancement can induce local nuclear fields of up to 1.0 T that can be observed as Zeeman splittings of the exciton recombination photoluminescence line.<sup>33</sup> In a previous study of the 2DES in Al<sub>x</sub>Ga<sub>1-x</sub>As/GaAs heterostructures, magnetoresistance detection of ESR (Ref. 34) was used to measure microwave DNP induced Overhauser shifts as large as 430 mT.<sup>35,36</sup>

## II. ELECTRICALLY DETECTED ESR EXPERIMENTS

We have employed magnetoresistance ( $\rho_{xx}$ ) detection to obtain ESR spectra<sup>34</sup> in three different Al<sub>x</sub>Ga<sub>1-x</sub>As/GaAs

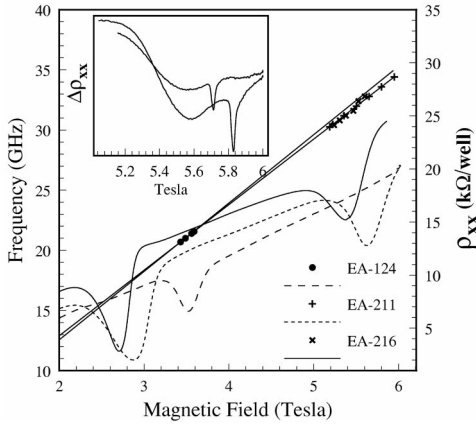


FIG. 1. Summary of transport detected ESR data near  $\nu=1$ ,  $T=2.4$  K in three different samples: EA-124, EA-211, and EA-216. Plots of  $\rho_{xx}$  correspond to the axis at right. The electrically detected ESR spectra at two different microwave frequencies are shown in the inset.

multiple quantum well samples, namely, EA-124, EA-216, and EA-221. These samples have 2D electron densities ranging from  $7.0 \times 10^{10}$  (EA-124) to  $1.6 \times 10^{11} \text{ cm}^{-2}$  (EA-221) and 4.2-K mobilities in the  $5 \times 10^5 \text{-cm}^2/\text{V s}$  range. Contacts to the 100- $\mu\text{m}$ -wide Hall bar pattern were made using  $\text{Au}_x\text{Ge}_{1-x}\text{N}$ . A second unpatterned sample from wafer EA-124 was set aside for the NMR experiments, to be discussed later. We will concentrate on the results from EA-124, since the enhancement of  $\langle I_z \rangle$  due to optical DNP was detected by both NMR and via the Overhauser shift in this sample under similar conditions. Sample EA-124 has a capping layer of 10 nm GaAs and 100 nm of  $\text{Al}_{0.1}\text{Ga}_{0.9}\text{As}$ , quantum well widths of 30 nm, and barrier widths of 360 nm. The 2D electrons were introduced by Si  $\delta$  doping in the center of the barrier.

For the microwave generation we employed a yttrium iron garnet (YIG) oscillator tunable over the 10–18 GHz range with an output power of 100 mW and a single frequency bandwidth of 1 MHz. A solid-state doubling amplifier produced  $>100$  mW microwave power in the 20–36 GHz range. For lock-in detection of the  $\Delta\rho_{xx}$  change due to ESR absorption, the microwaves were amplitude modulated. A gear-driven goniometer stage was employed for rotation of the samples to obtain the  $\rho_{xx}$  minimum at  $\nu=1$ , while maintaining the ESR frequency within the range of the microwave system. The microwave field was introduced through a coaxial transmission line terminated by a loop antenna. The  $\rho_{xx}$  and  $\Delta\rho_{xx}$  signals were simultaneously recorded using an injection current of 1–3  $\mu\text{A}$ . The ESR spectra were recorded by monitoring  $\Delta\rho_{xx}$  at constant microwave frequency, while sweeping the external magnetic field at a typical rate of 3 mT/s. The ESR data presented here were collected using either the Keck resistive magnet or the 100-mm 6-T superconducting magnet, both of which are located at the NHMFL.<sup>37</sup> The  $^4\text{He}$  bath temperature was determined from the vapor pressure and from a calibrated 100- $\Omega$  carbon film resistor mounted 1 cm above the sample.

A summary of our ESR data near  $\nu=1$  is presented in Fig. 1. The  $\rho_{xx}$  and  $\Delta\rho_{xx}$  magnetic field traces are plotted on the same abscissa. In EA-124,  $|g|=0.41$  was obtained, while in the higher density samples EA-216 and EA-221,  $|g|$

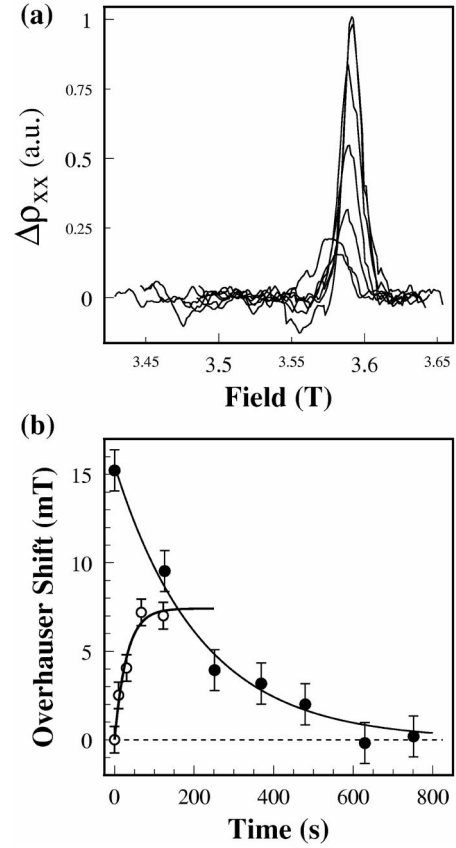


FIG. 2. Sample EA-124 data near  $\nu=1$  at  $T=2.4$  K. (a) Electrically detected ESR spectra recorded as a function of time following exposure to unpolarized light, as described in the text. In each case the nuclear relaxation was followed by repeated  $B_0$  up-sweeps. (b) Open circles,  $B_n(t)$  pumping due to exposure to unpolarized light, as described in the text. Filled circles, relaxation decay of  $B_n$  following optical excitation (see text).

$=0.39$ . This decrease in magnitude of the  $g$  factor with increasing magnetic field is in agreement with previous measurements in single heterostructures.<sup>38</sup> The detection sensitivity is estimated to be  $10^4$  spins/G.

To observe the optical DNP enhancement of the Overhauser shift, the samples were illuminated through a 600- $\mu\text{m}$ -diameter optical fiber mounted 1 cm above the sample. The diameter of the unpolarized output light spot on the sample was  $\approx 4\text{--}5$  mm. Figure 2(b) shows the experimental dependence of the induced local nuclear field  $B_n(t)$  upon exposure of sample EA-124 to an unpolarized  $\lambda=800$  nm light with a power density of  $\mathcal{I}=240 \text{ mW/cm}^2$ . The time dependence  $B_n(t) \propto \langle I_z \rangle$  can be derived assuming that cross relaxation between the electron spins of the 2DES and the nuclear spins is dominated by fluctuations of the scalar hyperfine interaction.<sup>20,29,30,35</sup> Ignoring the relatively small thermal equilibrium contribution to the nuclear spin polarization, and neglecting spin diffusion (valid for short pumping times),  $\langle I_z \rangle$  obeys

$$\frac{\langle I_z \rangle(t)}{I_0} = \frac{g \gamma_e}{\gamma_n} \left( \frac{\langle S_z \rangle - S_0}{S_0} \right) \left( 1 + \frac{T_{IS}}{T_{1n}} \right)^{-1} \times \{1 - \exp[-t(T_{IS}^{-1} + T_{1n}^{-1})]\}, \quad (2)$$

where  $1/T_{IS}$  is the electron-nuclear cross-relaxation rate,  $T_{1n}$  is the nuclear spin lattice relaxation time in the absence of light, and  $I_0$  is the nuclear spin polarization at thermal equilibrium. Equation (2) is independent of the statistics obeyed by the electrons and applies equally well for paramagnetic ions or electrons in a 2D metal.<sup>20,35</sup> A least-squares fit to Eq. (2), represented as the solid curve in Fig. 2(b), yielded a polarization time constant of 30 s.

There are several noteworthy features of Eq. (2) in its application to a 2DES. First, the thermal equilibrium spin polarization of the electrons in the 2DES,  $S_0$ , is now filling factor dependent, but  $S_0 \geq 0$  since  $g < 0$ . In the case of unpolarized light,  $\langle S_z \rangle \rightarrow 0$  when equal numbers of  $m_s = \pm 1/2$  electrons are excited, and the enhancement factor is given by the ratio of the electron and nuclear Larmor frequencies,  $g\gamma_e/\gamma_n$ . Since  $\gamma_e g > 0$  in GaAs and  $\gamma_n > 0$  for all three isotopes,  $\langle I_z \rangle < 0$ . In this case,  $B_n > 0$ , and the effect can be viewed as a  $(B_0 + B_n)/B_0$  enhancement of the  $g$  factor. Second, Eq. (2) reveals the possibility for suppression of  $E_z$  by optical DNP. The electron spin polarization  $\langle S_z \rangle$  is determined by the electric dipole transition matrix elements of the direct interband transitions near the center of the Brillouin zone, and  $S_0$  is the thermal equilibrium electron spin polarization. This establishes  $\langle S_z \rangle = \mp 1/4$  for  $\sigma^\pm$  (right or left circularly polarized) pumping light in bulk GaAs. Equation (2) implies that optical DNP can, under certain conditions, provide a suppression of the Zeeman energy, in contrast to microwave DNP, which can only produce a positive enhancement in GaAs.

The decay of  $B_n$  due to nuclear spin lattice relaxation following a fixed 154-s exposure of EA-124 to unpolarized light ( $\lambda = 784$  nm,  $\mathcal{I} = 180$  mW/cm<sup>2</sup>) is shown in Fig. 2. Figure 2(a) presents the ESR spectra, after subtraction of the nonresonant background contribution to  $\Delta\rho_{xx}$ , as a function of the post-excitation delay. The decay of the Overhauser shift, determined from the field displacement of the ESR maximum from the thermal equilibrium position, is shown in Fig. 2(b). The least-squares fit to this data by a single exponential is represented by the solid decay curve of Fig. 2(b). It should be noted that the relaxation decay time of  $T_{1n} = 214$  s does not correspond to the relaxation time at a single magnetic field (or filling factor) but rather to a value averaged over the entire range of filling factors covered by the sweep. From Fig. 2(a) it is apparent that the ESR peak intensity decreases and broadens with increasing time as the Overhauser shift decays back to its thermal equilibrium value. This can be accounted for by inhomogeneous broadening due to several possible sources. The optical field in this multiple quantum well sample will be most intense for quantum wells near the surface of the sample and, due to optical absorption, least intense for wells furthest away. Thus, the nuclear spin polarization varies from one well to the next, while we detect the ESR signal from all of the wells. In addition, variations of the nuclear spin polarization within each well can also occur due to the variation in  $|\psi(r)|^2 \langle I_z \rangle(r)$  [see Eq. (1)] across the well. The use of single quantum well samples in future experiments should help identify the source of the broadening.

In comparison with the 15-mT optical DNP enhancement of the Overhauser shift, a greater Overhauser shift would be induced by saturation of the ESR transition by resonant mi-

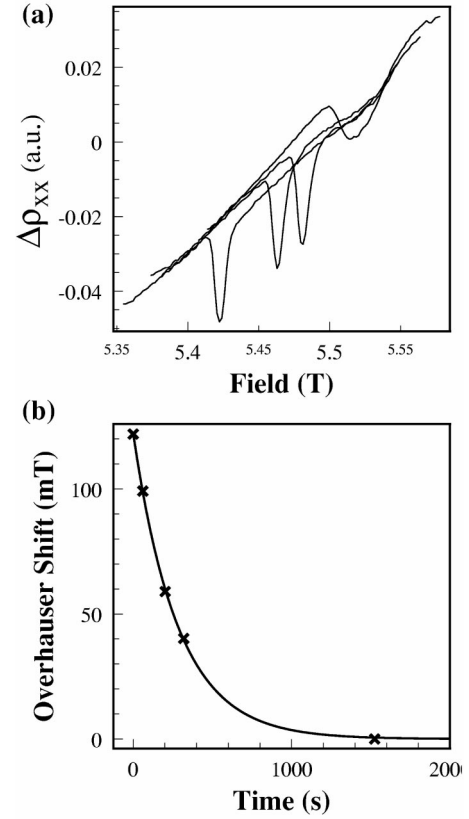


FIG. 3. Sample EA-124 data near  $\nu = 1$  at a temperature near 2.4 K. (a) Electrically detected ESR spectra acquired as a function of time following down-swept resonant microwave DNP. A maximum Overhauser shift of 120 mT was induced. (b) Decay of Overhauser shift of the ESR transition following down-swept microwave DNP.

crowaves, as demonstrated in Fig. 3. A maximum Overhauser shift of  $B_n = +120$  mT was observed using  $\approx 50$  mW microwave power at the source. The power at the sample is estimated to be on the order of a few mW. The Overhauser shift of the ESR to lower magnetic field is in the same direction as the shift obtained by unpolarized optical excitation. The decay of the Overhauser shift was fit to a single exponential, represented as the solid curve in Fig. 3(b). The decay constant of  $T_{1n} = 280$  s is comparable to the relaxation time found for the decay of the Overhauser shift following optical DNP, as described above.

## II. NMR EXPERIMENTS

Additional information about the local nuclear field induced by optical DNP can be obtained from radio-wave detected NMR experiments.<sup>2-4,30,31</sup> To eliminate any background NMR signal due to the GaAs substrate, the substrate was removed by chemical etching. The  $\text{Al}_{0.1}\text{Ga}_{0.9}\text{As}/\text{GaAs}$  multiquantum well film was then transferred to a silicon substrate and fixed with epoxy. The NMR data were collected at a fixed field of 3 T in a high homogeneity Oxford superconducting magnet. A typical optical DNP-enhanced  $^{71}\text{Ga}$  NMR spectrum is shown in Fig. 4(d). No Knight shift was observed at 4.2 K, presumably due to the relatively high temperature and low electron density of this sample. Three NMR lines are observed, each with a linewidth of  $\sim 3$  KHz (FWHM) and separated by 55 kHz. The splitting is due to a

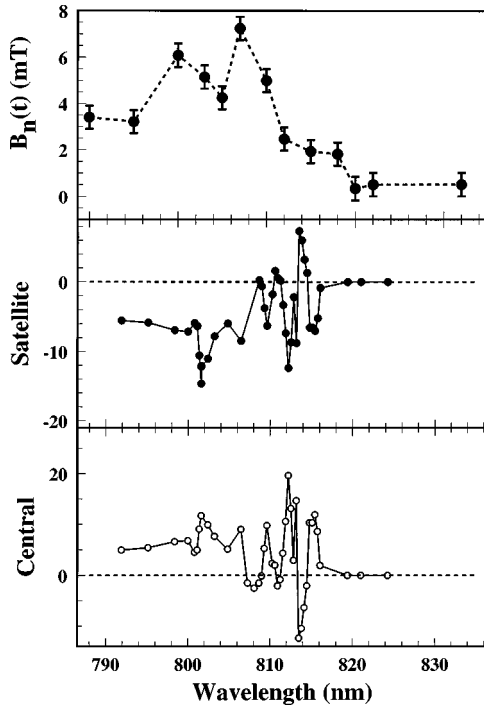


FIG. 4. (a) Wavelength dependence of the  $B_n$  enhancement by optical DNP in EA-124 at 2.4 K, with  $\mathcal{I}=106$  mW/cm<sup>2</sup>. The data were collected at  $B_0=3.3$  T, near  $\nu=1$ . The wavelength dependence of the central and satellite NMR transition amplitudes are shown in (b),(c), respectively, for sample EA-124 at  $B_0=3.0$  T,  $T=4.2$  K,  $\mathcal{I}=800$  mW/cm<sup>2</sup>.

strain-induced nuclear quadrupole interaction caused by the difference in the thermal expansion coefficients of the film and the Si support. Due to the  $\approx 20$   $\mu$ s dead time of the receiver, it was necessary to extrapolate each complex free induction decay to the origin of time defined by the termination of the 1.5- $\mu$ s rf detection pulse. This procedure eliminates the phase shift proportional to the rotating frame frequency offset. The NMR signal is predominantly due to nuclei in the GaAs quantum well regions. With longer optical pumping times, the central peak is seen to grow disproportionately due to spin diffusion into the Al<sub>0.1</sub>Ga<sub>0.9</sub>As regions. The satellite transitions cannot spin diffuse into the barriers due to the mismatch in transition energy with the Al<sub>0.1</sub>Ga<sub>0.9</sub>As satellites, which experience a substantial first order quadrupole broadening due to the presence of 10% aluminum.<sup>39</sup> This spectral assignment is confirmed by comparing the known composition of the film with the thermal equilibrium NMR spectrum shown in Fig. 4(e). The enhancement by optical DNP of the satellite and central NMR transitions varies dramatically with wavelength, as demonstrated in Figs. 4(b) and 4(c). For instance, the spectra of Figs. 5(a) and 5(b) show that a 180° phase inversion occurs upon changing the excitation wavelength by only 0.335 nm (150 GHz). These inversions are probably due to spin state selective optical pumping in the lowest two Landau levels. Also note the antiphase relationship between the satellite and central peaks, which is observed over the entire wavelength range. The antiphase NMR line shape is consistent with the existence of an octupole polarization with an admixture of dipole polarization. The NMR phase inversions cease to

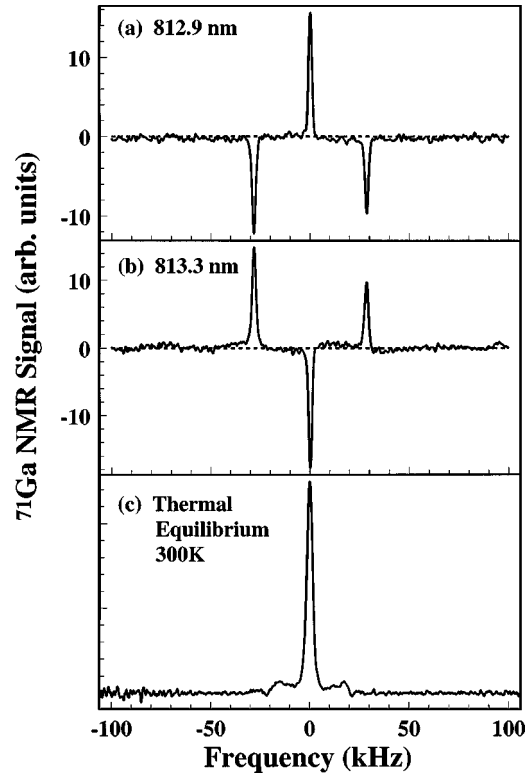


FIG. 5. Fourier transform NMR spectra of <sup>71</sup>Ga in the film sample EA-124. (a) and (b) spectra obtained at 4.2 K using a 1.5- $\mu$ s resonant radio-frequency pulse following a 40-s period of optical irradiation at  $\lambda=812.9$  and 813.3 nm, respectively. (c) NMR spectrum of the EA-124 film obtained at 300 K after averaging 30 000 free-induction decays. The weak satellite transitions of the GaAs layers at  $\pm 15$  kHz may be seen under careful inspection.

occur at shorter wavelength, and simultaneously, the Overhauser shift abruptly increases.

### III. ESTIMATION OF THE HYPERFINE COUPLING

It is interesting to compare the wavelength dependence of the optical DNP-induced local nuclear field  $B_n$ , as detected by the Overhauser shift of the electrically detected ESR signal, with the wavelength dependence of the optical DNP enhancement of the radio-wave-detected NMR signal. As is apparent from Fig. 4(a), there is no reversal of the sign of the Overhauser shift at any wavelength. This indicates that the total hyperfine nuclear field summed over all NMR transitions of all three isotopes does not invert.

We note that by measuring the nuclear spin polarization and Overhauser shift under identical experimental conditions in the same sample, an estimate of the hyperfine coupling constant can be obtained. The polarization of the central transition following a 40-s optical excitation at 801.5 nm is estimated to be  $\langle I_z \rangle = 3.2 \times 10^{-3}$ , which corresponds to the observed signal enhancement factor of 1050 over the thermal equilibrium signal [Fig. 5(c)] at 300 K. Under similar optical DNP conditions, an Overhauser shift of  $B_n = 6$  mT is observed, which establishes  $B_n = -3.7 \langle I_z \rangle$  as the collective hyperfine coupling constant between the conduction 2DES and quantum well nuclei, taking into account the contribution due to all three isotopes.<sup>26</sup> We hypothesize that a larger value

would result if not for the destructive interference between hyperfine field components. The estimated hyperfine coupling constant for this 2DES is remarkably close to the theoretical estimate of 3.53 T for the shallow donor trapped electrons in bulk GaAs.<sup>26,35</sup>

#### IV. CONCLUSIONS

In summary, we have demonstrated that the effective Zeeman energy of a 2DES near  $\nu=1$  can be enhanced by optical DNP with unpolarized light. Although the maximum observed Overhauser shift was only about 15 mT, increased optical intensities, longer pumping times, and a judicious choice of the pumping field to minimize spin-lattice relaxation is expected to substantially increase this value. Zeeman energy enhancement under optical DNP conditions may be

applied to NMR studies of the QHE.<sup>2-4</sup> For example, optical DNP may be useful as a method for suppression of the Zeeman energy in order to enhance the number of spin flips involved in Skyrmionic excitations in the quantum Hall effect.

#### ACKNOWLEDGMENTS

We thank N. Bonesteel, L. Engel, J. Graybeal, and I. Kukushkin for helpful discussions, B.-J. Pullum and M. Whitton for technical assistance, and B. Brandt, for operational assistance at the NHMFL'S resistive magnet facility. This work was supported by NSF Grant No. CHE-9624243 and U.S. DOE Contract No. DE-AC04-94AL85000. The NHMFL is supported by NSF Cooperative Agreement No. DMR-9527035 and by the State of Florida.

\*Present address: Physics Department, City College of New York, Convent Avenue at 138th Street, New York, NY 10031.

†Author to whom correspondence should be addressed.

<sup>1</sup>For a review of the electronic properties of two-dimensional systems, see T. Ando, A. Fowler, and F. Stern, *Rev. Mod. Phys.* **54**, 437 (1982).

<sup>2</sup>S. E. Barrett, G. Dabbagh, L. N. Pfeiffer, K. W. West, and R. Tycko, *Phys. Rev. Lett.* **74**, 5112 (1995).

<sup>3</sup>R. Tycko, S. E. Barrett, G. Dabbagh, L. N. Pfeiffer, and K. W. West, *Science* **268**, 1460 (1995).

<sup>4</sup>N. N. Kuzma, P. Khandelwal, S. E. Barrett, L. N. Pfeiffer, and K. W. West, *Science* **281**, 686 (1998).

<sup>5</sup>A. Schmeller, J. P. Eisenstein, L. N. Pfeiffer, and K. W. West, *Phys. Rev. Lett.* **75**, 4290 (1995).

<sup>6</sup>E. H. Aifer, B. B. Goldberg, and D. A. Broido, *Phys. Rev. Lett.* **76**, 680 (1996).

<sup>7</sup>V. Bayot, E. Grivei, S. Melinte, M. B. Santos, and M. Shayegan, *Phys. Rev. Lett.* **76**, 4584 (1996); **79**, 1718 (1997).

<sup>8</sup>I. V. Kukushkin, K. von Klitzing, and K. Eberl, *Phys. Rev. B* **55**, 10 607 (1997).

<sup>9</sup>S. L. Sondhi, A. Karlhede, S. A. Kivelson, and E. H. Rezayi, *Phys. Rev. B* **47**, 16 419 (1993).

<sup>10</sup>H. A. Fertig, L. Brey, R. Côté, and A. H. MacDonald, *Phys. Rev. B* **50**, 11 018 (1994).

<sup>11</sup>J. K. Jain and X. G. Wu, *Phys. Rev. B* **49**, 5085 (1994).

<sup>12</sup>D. K. Maude, M. Potemski, J. C. Portal, M. Henini, L. Eaves, G. Hill, and M. A. Pate, *Phys. Rev. Lett.* **77**, 4604 (1996).

<sup>13</sup>C. Weisbuch and C. Hermann, *Phys. Rev. B* **4**, 1296 (1971).

<sup>14</sup>The effect of a tilted field on a two-dimensional electron gas was first investigated by F. F. Fang and P. J. Stiles, *Phys. Rev.* **174**, 823 (1968).

<sup>15</sup>The effect of a tilted field on the fractional quantum Hall effect was first investigated by R. J. Haug *et al.*, *Surf. Sci.* **196**, 242 (1988).

<sup>16</sup>J. P. Eisenstein, H. L. Stormer, L. Pfeiffer, and K. W. West, *Phys. Rev. Lett.* **62**, 1540 (1989).

<sup>17</sup>R. G. Clark, S. R. Haynes, A. M. Suckling, J. R. Mallett, P. A. Wright, J. J. Harris, and C. T. Foxon, *Phys. Rev. Lett.* **62**, 1536 (1989).

<sup>18</sup>L. W. Engel, S. W. Hwang, T. Sajoto, D. C. Tsui, and M. Shayegan, *Phys. Rev. B* **45**, 3418 (1992).

<sup>19</sup>V. Melik-Alaverdian, N. E. Bonesteel, and G. Ortiz, *Phys. Rev. B* (to be published).

<sup>20</sup>A. Abragam, *Principles of Nuclear Magnetism* (Clarendon, Oxford, 1987).

<sup>21</sup>A. W. Overhauser, *Phys. Rev.* **91**, 476 (1953).

<sup>22</sup>Y. Yaffet, *Solid State Phys.* **14**, 92 (1963).

<sup>23</sup>C. P. Slichter, *Principles of Magnetic Resonance*, Springer Series in Solid State Sciences Vol. 1 (Springer-Verlag, Berlin, 1978).

<sup>24</sup>G. Lampel, *Phys. Rev. Lett.* **20**, 491 (1968).

<sup>25</sup>A. I. Ekimov and V. I. Safarov, *Zh. Éksp. Teor. Fiz., Pis'ma Red.* **15**, 257 (1972) [*JETP Lett.* **15**, 179 (1972)].

<sup>26</sup>D. Paget, G. Lampel, B. Sapoval, and V. I. Safarov, *Phys. Rev. B* **15**, 5780 (1977).

<sup>27</sup>S. E. Barrett, R. Tycko, L. N. Pfeiffer, and K. W. West, *Phys. Rev. Lett.* **72**, 1368 (1994).

<sup>28</sup>J. A. Marahn, P. J. Carson, J. Y. Hwang, M. A. Miller, D. N. Shykind, and D. P. Weitekamp, *Phys. Rev. Lett.* **75**, 1364 (1995).

<sup>29</sup>P. L. Kuhns, A. Kleinhammes, T. Schmiedel, W. G. Moulton, P. Chabrier, S. Sloan, E. Hughes, and C. R. Bowers, *Phys. Rev. B* **55**, 7824 (1997).

<sup>30</sup>C. R. Bowers, *Solid State Nucl. Magn. Reson.* **11**, 11 (1998).

<sup>31</sup>M. I. D'yakonov and V. I. Perel', *Zh. Éksp. Teor. Fiz.* **65**, 362 (1973) [*Sov. Phys. JETP* **38**, 177 (1974)].

<sup>32</sup>F. Meier and B. P. Zakharchenya, *Optical Orientation* (North-Holland, Amsterdam, 1984), and references therein.

<sup>33</sup>S. W. Brown, T. A. Kennedy, D. Gammon, and E. S. Snow, *Phys. Rev. B* **54**, R17 339 (1996).

<sup>34</sup>D. Stein, K. von Klitzing, and G. Weimann, *Phys. Rev. Lett.* **51**, 130 (1983).

<sup>35</sup>M. Dohers, K. v. Klitzing, J. Schneider, G. Weimann, and K. Ploog, *Phys. Rev. Lett.* **61**, 1650 (1988).

<sup>36</sup>A. Berg, M. Dohers, R. R. Gerhardt, and K. v. Klitzing, *Phys. Rev. Lett.* **64**, 2563 (1990).

<sup>37</sup>National High Magnetic Field Laboratory, 1800 E. Paul Dirac Drive, Tallahassee, Florida 32310.

<sup>38</sup>M. Dohers, K. von Klitzing, and G. Weimann, *Phys. Rev. B* **38**, 5453 (1988).

<sup>39</sup>V. L. Berkovits and V. I. Safarov, *Fiz. Tverd. Tela (Leningrad)* **20**, 2536 (1978) [*Sov. Phys. Solid State* **20**, 1468 (1978)].